min, the synaptosome-rich interface was removed and recentrifuged to remove any remaining Ficoll.

RNA Interference—Stealth™ small interfering RNA (siRNA) duplex oligoribonucleotides against PC12 cell TrkA (GenBank™ number NM_021589) and the p75 neurotrophin receptor (p75^{NTR}) (GenBank™ number NM_012610) were synthesized by Invitrogen. The siRNA sequences used were as follows: rTrkA-siRNA (position 1370) sense (5′-GCCCUCCUCCUAGUGCUCAACAAAU-3′) and antisense (5′-AUUUGUUGAGCACUAGGAGGAGGGC-3′); rTrkA-siRNA-control sense (5′-GCCCUCCGAUCUCGUCAACAUCAAU-3′) and antisense (5′-AUUGAUGUUGACGAGAUCGGAGGGC-3′); rp75-siRNA (position 1212) sense (5′-CAGCCUGAACAUAUAGACUCCUUUA-3′) and antisense (5′-UAAAGGAGUCUUAUAUGUUCAGGCUG-3′); rp75-siRNA-control sense (5′-CAGGUAAACAUAUAGUCCCUCCUUA-3′) and antisense (5′-UAAGGAGGGACUAUAUGUUUACCUG-3′). The control siRNA had a random sequence. siRNA oligonucleotides were transfected into PC12 cells using Lipofectamine 2000 (Invitrogen) according to the manufacturer's protocol.

RESULTS

Toxicity of Aβ Assembly Formed from Arctic-type Aβ—We treated primary neurons with seed-free wild- or Arctic-type Aβ, which had been preincubated for 2 h in the absence or presence of GM1 ganglioside (10 or 20% molar ratio in the lipids composing liposomes). Unexpectedly, extensive neuronal death was observed in the culture treated with Arctic-type Aβ, which had been preincubated for 2 h in the presence of GM1 ganglioside at a 10% molar ratio in liposomes (Fig. 1*A*). The extent of neuronal death under this condition was greater than that under any other conditions examined in this study (Fig. 1, *A* and *B*).

To quantitatively characterize the toxic Aβ assembly, we examined its toxicity against NGF-treated PC12 cells (PC12N cells). We found that PC12N cells are also sensitive to the toxic Aβ assembly formed from Arctic-type Aβ (Fig. 1*C*). We performed an LDH release assay of cultures of PC12N cells under various conditions. The level of LDH released from the PC12N cells, which were treated with the toxic Aβ assembly, increased depending on Aβ dose (Fig. 1*D*), GM1 ganglioside dose (Fig. 1*E*), and the duration of the exposure of the cells to the toxic Aβ assembly (Fig. 1*F*). In regard to the time course of Aβ preincubation with GM1 ganglioside, the level of released LDH increased with peak value at 2 h and then decreased in conjunction with an increase in the ThT fluorescence intensity of the incubation mixtures (Fig. 1*G*).

The Toxic Aβ Assembly Is Soluble—Importantly, the toxicity of the Aβ incubated in the presence of GM1 ganglioside was observed exclusively in the supernatant obtained by ultracentrifuging the incubation mixture (Fig. 2*A*), suggesting that the toxic Aβ assembly is soluble. To examine the possibility that a TAβ is formed in the presence GM1 ganglioside, we performed dot blotting using an oligomer-specific antibody (anti-Oligo) (23). TAβ in the incubation mixtures was readily recognized by anti-Oligo (Fig. 2*B*). The specificity of TAβ recognition by anti-Oligo was confirmed by the finding that TAβ toxicity was significantly neutralized by coincubating the mixtures with anti-Oligo in the cultures of PC12N cells and primary neurons (Fig. 2*C*). However, coincubation with a monoclonal antibody (4396C), which inhibits Aβ fibrillogenesis through binding to GM1 ganglioside-bound Aβ as a seed (40), failed to inhibit the induction of TAβ toxicity (Fig. 2*D*).

TAβ Formation from Wild-type Aβ—We then examined whether TAβ is also formed from wild-type Aβ (Aβ40). We first investigated how TAβ is formed from wild-type Aβ in the presence of liposomes containing GM1 ganglioside. Interestingly, TAβ is favorably formed from wild-type Aβ in the presence of GM1 ganglioside at a 15% molar ratio in liposomes (Fig. 3*A*). TAβ toxicity was not significant in the nanomolar range of Aβ (Fig. 3*B*).

Biophysical and Structural Features of TAβ—To determine the biophysical and structural features of TAβ, we performed SDS-PAGE of the incubation mixtures containing TAβ. However, no high molecular weight bands corresponding to possible Aβ assemblies were detected. Bands were observed only after cross-linking pretreatment with glutaraldehyde (Fig. 4*A*), consistent with previous findings showing that soluble Aβ assemblies are probably degraded by denaturing gel electrophoresis (6) unless they are cross-linked (44, 45). A morphological analysis of TAβ by electron microscopy failed to detect any definite structure under conditions in which protofibrils, which had been prepared as previously reported (30), were readily detectable (Fig. 4*B*). In contrast, spherical particles with diameters of 10–20 nm, along with rod-shaped structures, were observed by AFM in the supernatant obtained by ultracentrifuging the incubation mixtures containing TAβ (Fig. 4*C*). We then determined the molecular mass of TAβ by size exclusion chromatography, which was followed by dot blotting using anti-Oligo. The immunoreactivity was recovered as a single peak with relative molecular masses of 200–300 kDa (Fig. 4*D*). The recovery of TAβ immunoreactivity in the same fraction was also observed in the incubation mixture containing wild-type Aβ (Aβ40) and GM1 ganglioside at a 15% molar ratio in liposomes (Fig. 4*D*). Furthermore, the collected peak showed a significant toxicity against PC12N cells (Fig. 4*E*).

TAβ Formation in the Presence of Natural Neuronal Membranes—Next, we tested whether TAβ can be formed in the presence of natural neuronal membranes. We incubated Arctic-type Aβ in the presence of synaptosomes prepared from brains of mice from three different age groups. The degree of TAβ formation was significantly higher in the incubation mixture containing synaptosomes prepared from the hippocampus of aged (2-year-old) mouse brains than in any other incubation mixtures, including those containing synaptosomes from the hippocampus or the whole brain minus the hippocampus from younger (1-month-old and 1-year-old) mouse brains (Fig. 5*A*). To determine the possibility that an alteration in the lipid composition of neuronal membranes, particularly GM1 ganglioside, underlies the acceleration of TAβ formation, we determined the levels of GM1 ganglioside, cholesterol, and phospholipids in synaptosomes prepared from hippocampi of young (1-month-old) and aged (2-year-old) mouse brains. Notably, the GM1 ganglioside level significantly increased, whereas cholesterol level significantly decreased with age (Fig. 5*B*).

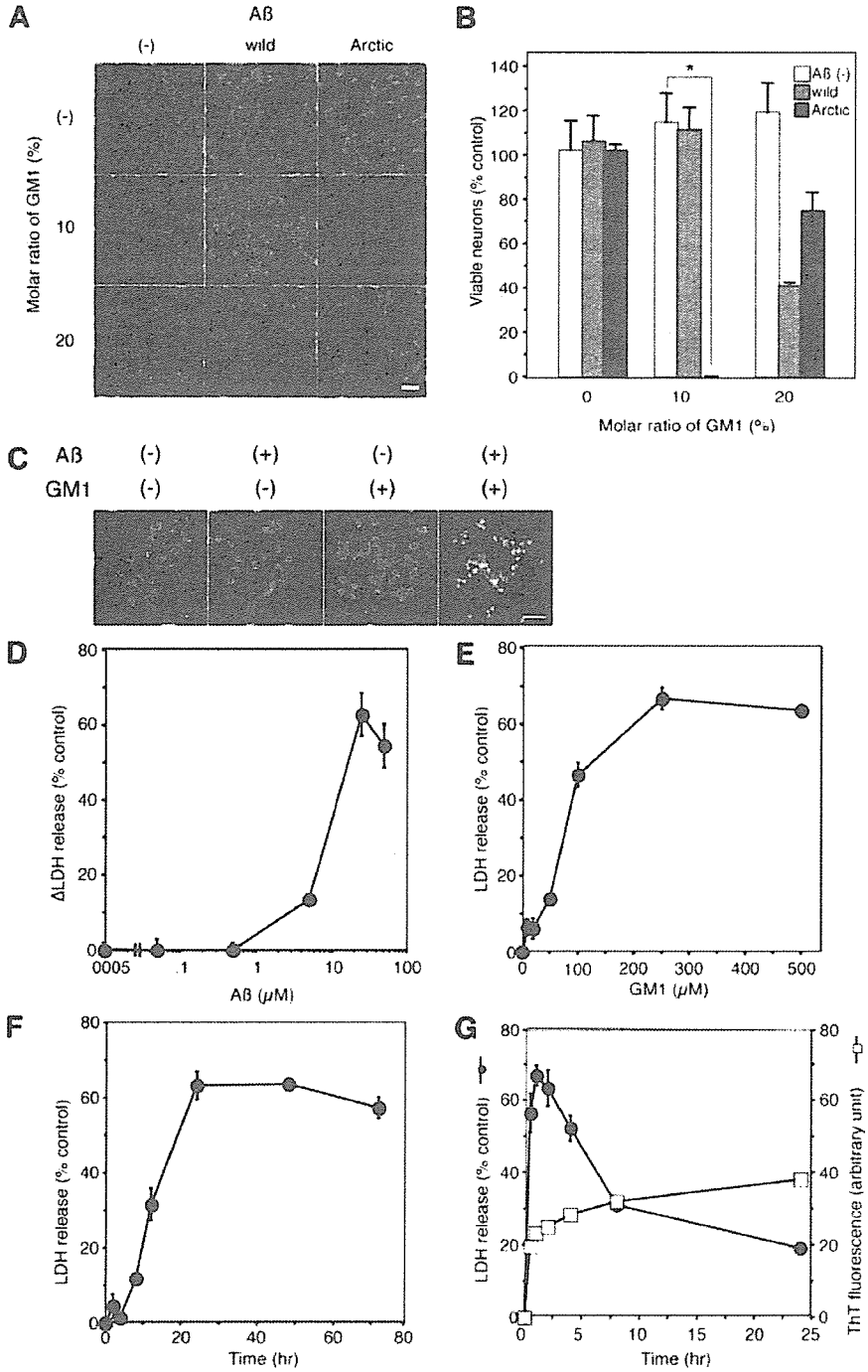

FIGURE 1. **Toxicity of Aβ assembly formed in the presence of GM1 ganglioside against primary neurons and PC12N cells.** *A*, primary cortical neurons cultured for 48 h in serum-free N2-supplemented medium were treated at 37 °C for 48 h with incubation mixtures containing seed-free wild-type Aβ (Aβ40) or Arctic-type Aβ (Aβ40) at a final concentration of 25 μM, which had been preincubated at 50 μM and 37 °C for 2 h in the absence or presence of GM1 ganglioside-containing liposomes. The GM1 ganglioside concentration in the incubation mixtures was 500 μM; the molar ratio of GM1 ganglioside in liposomes varied as indicated. Neurons were stained with calcein AM (Invitrogen)/ethidium homodimer, showing green staining for viable cells and *red* staining for dead cells. *Bar*, 50 μm. *B*, the number of viable neurons in the culture shown in *A* was determined. Each *column* indicates the average of three percentages ± S.D. relative to that of control cultures in which neither Aβ nor GM1 ganglioside was added. *, $p < 0.0001$ (one-way analysis of variance combined with Scheffe's test). *C*, representative images of NGF-treated PC12 (PC12N) cells treated at 37 °C for 48 h with incubation mixtures containing Arctic-type Aβ (Aβ40) at a final concentration of 25 μM, which had been preincubated at 50 μM and 37 °C for 2 h in the absence or presence of GM1 ganglioside-containing liposomes. The GM1 ganglioside concentration in the incubation mixtures was 500 μM, and the molar ratio of GM1 ganglioside in liposomes was 10%. *Bar*, 50 μm. *D* and *E*, dose-response curves for the level of LDH released from cells treated with incubation mixtures containing Aβ, which had been preincubated as described in *C*. The concentrations of Aβ and GM1 ganglioside varied as indicated. The LDH value indicates the percentage level of LDH released following treatment with incubation mixtures relative to the level of LDH released following treatment with Triton X-100. *D*, the points indicate LDH levels in the incubation mixtures containing GM1 ganglioside minus those lacking GM1 gangliosides, which were negligible below 25 μM Aβ. *F* and *G*, time course curves for level of LDH released from the cells treated with incubation mixtures containing Aβ, which had been preincubated as described in *A*. The durations of cell treatment (*F*) and Aβ preincubation in the presence of GM1 ganglioside (*G*) varied as indicated. ThT fluorescence intensities in the incubation mixtures are also shown in *G*. *D–G*, each point indicates the average of four values ± S.D.

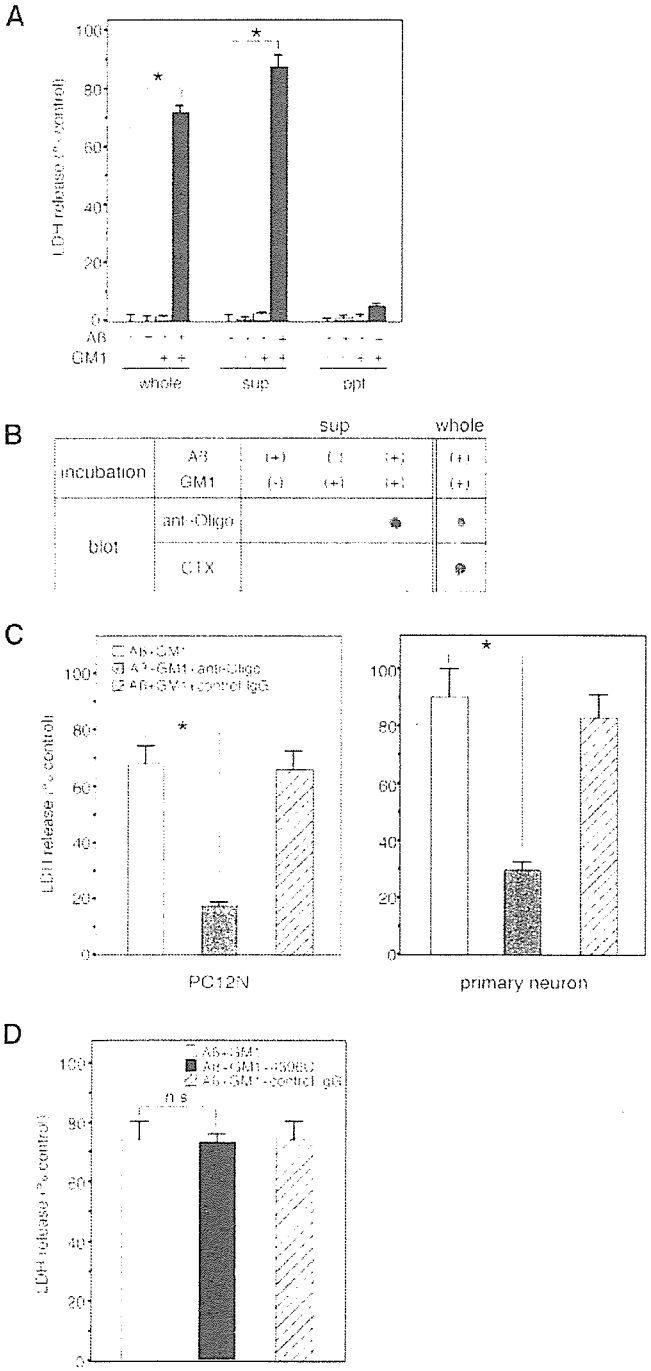

FIGURE 2. **Recognition of toxic Aβ assembly by oligomer-specific antibody.** *A*, the level of LDH released from PC12N cells treated at 37 °C for 48 h with supernatant (*sup*) or precipitate (*ppt*) obtained by ultracentrifuging (540,000 × *g*, 15 min) incubation mixtures (*whole*) containing Arctic-type Aβ (*Aβ40*) at final concentration of 25 μM, which had been preincubated at 50 μM and 37 °C for 2 h in the absence or presence of 500 μM GM1 ganglioside (the molar ratio of GM1 ganglioside in liposomes was 10%). Each value indicates the percentage level of LDH released following treatment with incubation mixtures relative to the level of LDH released following treatment with Triton X-100. Each *column* indicates the average of three values ± S.D. *, $p < 0.0001$. *B*, dot blot analysis of supernatant (*sup*) obtained by ultracentrifuging incubation mixtures (*whole*) containing Arctic-type Aβ alone, GM1 ganglioside alone, or Arctic-type Aβ plus GM1 ganglioside. The blots were reacted with anti-Oligo (BIOSOURCE Inc., Camarillo, CA) or cholera toxin subunit B-horseradish peroxidase conjugate (Sigma) (*CTX*). *C*, the level of LDH released from PC12N cells and primary neurons treated at 37 °C for 48 h with incubation mixtures containing Arctic-type Aβ (Aβ40) at a final concentration of 25 μM, which had been preincubated at 50 μM and 37 °C for 2 h in the presence of GM1 ganglioside and anti-Oligo. Each *column* indicates the average of three values ± S.D. *, $p < 0.0001$. *D*, the level of LDH released from PC12N cells treated at 37 °C for 48 h with Arctic-type Aβ, which had been preincubated in the presence of GM1 ganglioside and 4396C. Each column indicates the average of three values ± S.D. *n.s.*, not significant.

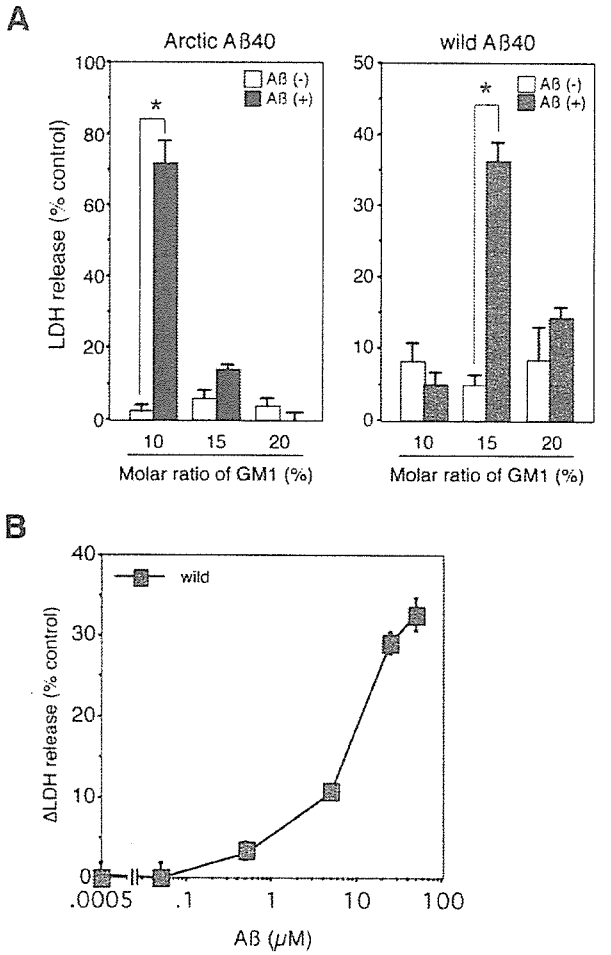

FIGURE 3. **TAβ formation from wild-type Aβ.** *A*, the level of LDH released from NGF-treated PC12 (PC12N) cells treated at 37 °C for 48 h with incubation mixtures containing Arctic-type Aβ (Aβ40), wild-type Aβ (Aβ40) at a final concentration of 25 μM, which had been preincubated at 50 μM for 2 h at 37 °C in the presence of GM1-ganglioside-containing liposomes. The GM1 ganglioside concentration in the incubation mixtures was 500 μM, and the molar ratio of GM1 ganglioside in liposomes varied as indicated. Each value indicates the percentage level of LDH released following treatment with incubation mixtures relative to the level of LDH released following treatment with Triton X-100. Each column indicates the average of three values ± S.D. *, $p < 0.0001$. *B*, the level of LDH released from PC12N cells treated at 37 °C for 48 h with incubation mixtures containing wild-type Aβ at various concentrations, which had been preincubated in the absence or presence of 500 μM GM1 ganglioside (the molar ratio of GM1 ganglioside in liposomes was 15%). Each point indicates the LDH level in the incubation mixtures containing GM1 ganglioside minus that of the incubation mixtures lacking GM1 gangliosides, which was negligible below 25 μM for wild-type Aβ.

Putative Mechanism Underlying TAβ-induced Neuronal Death—To characterize cell death induced by TAβ, we performed nuclear staining with a membrane-permeable dye, Hoechst 33258. PC12N cells, which were treated with incubation mixtures containing TAβ for 12 h, showed characteristics of apoptotic changes, including retracted neurites, shrunken

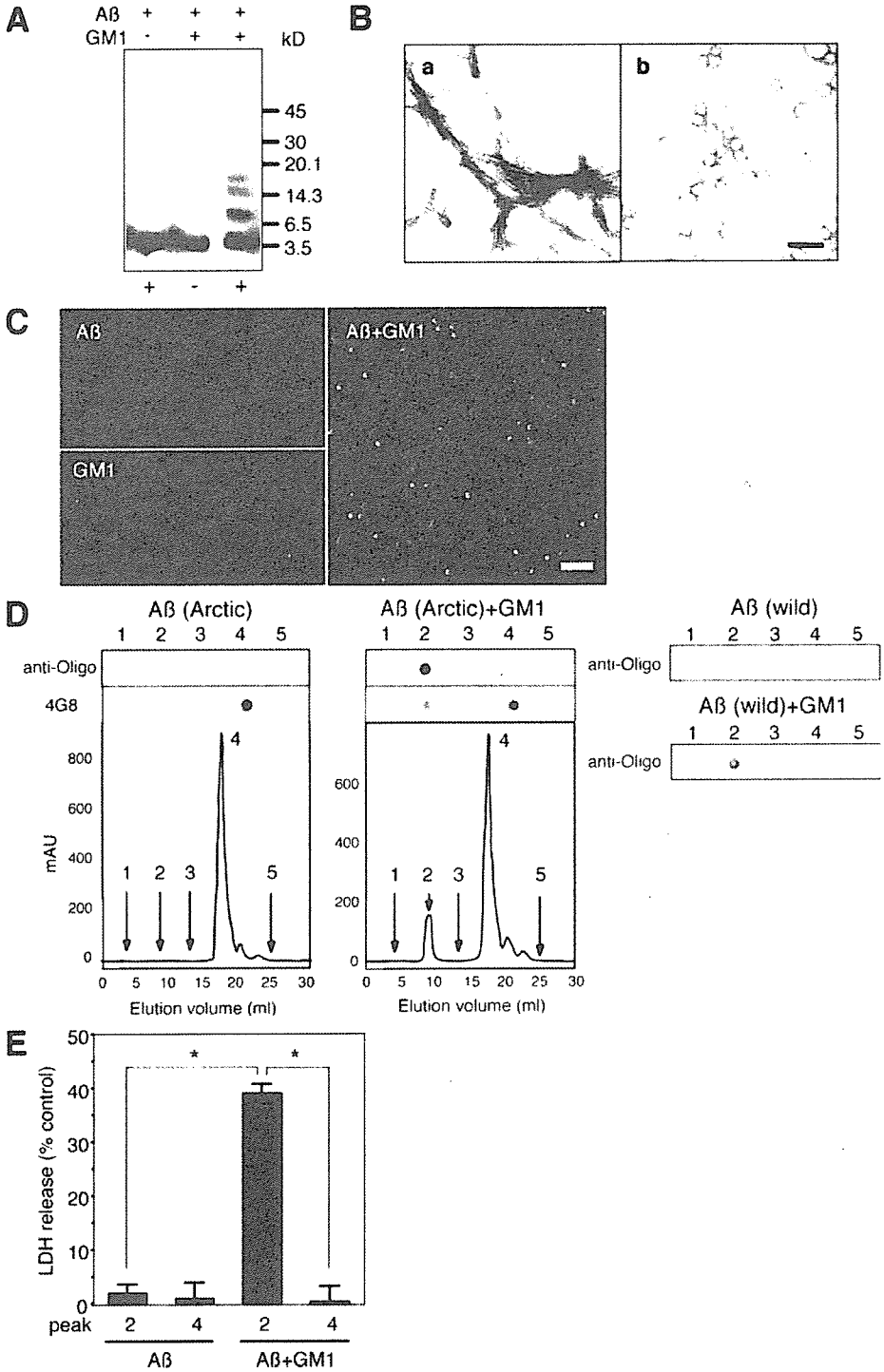

FIGURE 4. **Biophysical and structural analyses of TAβ.** *A*, Western blot of supernatants of incubation mixtures containing Arctic-type Aβ (Aβ40), which had been incubated at 50 μM and 37 °C for 24 h in the absence or presence of 500 μM GM1 ganglioside (the molar ratio of GM1 ganglioside in liposomes was 10%). Ten nanograms of Aβ in the incubation mixtures was subjected to SDS-PAGE (4–20% gradient gel) with (+) or without (−) cross-linking pretreatment using glutaraldehyde. The blot was reacted with 4G8. *B*, electron micrographs of incubation mixture containing Arctic-type Aβ preincubated to allow protofibril formation (*a*) or of incubation mixture containing TAβ formed from Arctic-type Aβ (*b*). Typical protofibril structures were observed in *a*; however, no definite structures aside from liposomes were observed in *b*. *Bar*, 100 nm. *C*, AFM image of fraction containing TAβ formed from Arctic-type Aβ. The supernatant obtained by ultracentrifuging (540,000 × *g*, 3 h) the incubation mixture containing TAβ was subjected to AFM. Spherical particles along with rod-shaped structures were observed. No definite structures were observed in the supernatants of incubation mixtures containing Arctic-type Aβ alone or GM1 ganglioside alone. The amplitude range is 0.1 V. *Bar*, 200 nm. *D*, size exclusion chromatography of incubation mixtures containing Aβ, which had been preincubated in the absence or presence of GM1 ganglioside, on a Superose 12 column. Elution samples from 35 fractions were dot-blotted on nitrocellulose membranes. The blot was reacted with anti-Oligo or 4G8. The immunoreactivity with anti-Oligo was recovered as a single peak with an apparent molecular mass of 200–300 kDa. Five representative fractions are shown. *Peaks 2* and *4* correspond to fractions containing TAβ and monomeric Aβ, respectively. *mAU*, milli-absorbance unit. *E*, toxicities of peaks (*2* and *4*) collected from incubation mixtures containing Arctic-type Aβ (shown in *D*) against PC12N cells. Each *column* indicates the average of three values ± S.D.*, $p < 0.0001$.

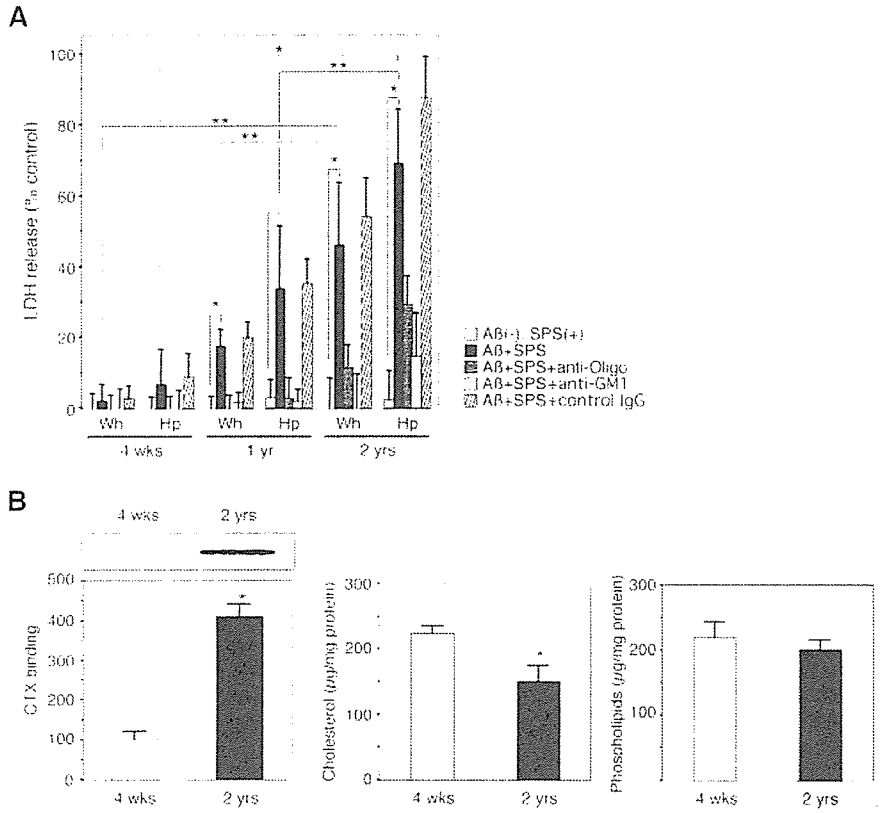

FIGURE 5. **TAβ formation from Arctic-type Aβ incubated in the presence of synaptosomes.** *A*, TAβ formation was assessed by LDH release assay of PC12N cell cultures treated at 37 °C for 48 h with incubation mixtures containing Arctic-type Aβ (Aβ40) at a final concentration of 25 μM, which had been preincubated at 50 μM and 37 °C for 2 h in the absence or presence of synaptosomes (*SPS*) prepared from brains of mice of three different age groups with or without anti-Oligo or an antibody specific to GM1 ganglioside (Calbiochem). *Wh*, whole brain minus hippocampus; *Hp*, hippocampus. Each *column* indicates the average of four values ± S.D. *, $p < 0.0001$; **, $p < 0.005$. *B*, lipid composition of synaptosomes prepared from young (1-month-old) and aged (2-year-old) mouse brains. GM1 ganglioside levels were determined by densitoscanning the blot following incubation with cholera toxin. Levels of cholesterol and phospholipids were determined using Determiner L (Kyowa, Tokyo, Japan) and phospholipids C (Wako, Osaka, Japan), respectively. Each *column* indicates the average of four values ± S.D. *, $p < 0.0001$.

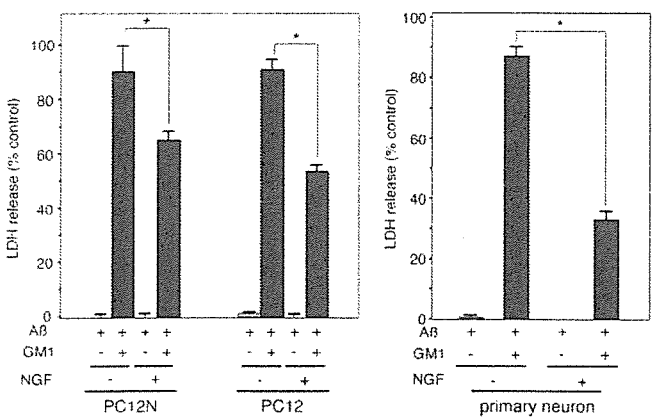

FIGURE 6. **Suppression of TAβ toxicity by the addition of exogenous NGF.** NGF-treated PC12 (PC12N), native PC12 cells, and primary neurons were treated with the incubation mixture containing Arctic-type Aβ (Aβ40) at a final concentration of 25 μM, which had been preincubated at 50 μM and 37 °C for 2 h in the absence or presence of 500 μM GM1 ganglioside (the molar ratio of GM1 ganglioside in liposomes was 10%) and exogenous NGF (100 ng/ml). TAβ toxicity was assessed by an LDH release assay in these cultures. Each *column* indicates the average of three values ± S.D. *, $p < 0.0001$.

cell bodies, and the condensation and fragmentation of nuclei in conjunction with an increase in the level of LDH released from TAβ-treated PC12N cells (data not shown). To determine if TAβ toxicity is mediated by NGF receptors, we first treated PC12N cells, native PC12 cells, and primary neurons with TAβ in the presence of exogenous NGF. In these cultures, cell death was markedly prevented (Fig. 6). We then knocked down the NGF receptors, including TrkA and $p75^{NTR}$, of PC12 cells, SY5Y cells, and primary neurons using specific siRNAs. The knockdown of $p75^{NTR}$ or TrkA markedly suppressed the cell death induced by TAβ in these cultures (Fig. 7).

DISCUSSION

Here, we show that a highly toxic soluble Aβ assembly (TAβ) can be formed more rapidly and to a greater extent from Arctic-type Aβ than from wild-type Aβ. Notably, TAβ formation requires GM1 ganglioside at certain densities. TAβ is probably formed via a pathway different from one that leads to amyloid fibril formation. Biophysical and structural analyses by AFM and size exclusion chromatography revealed that TAβ is spherical with diameters of 10–20 nm and molecular masses of 200–300 kDa. The most striking feature of TAβ is its unique toxicity. Our results suggest that TAβ induces the NGF receptor-mediated apoptosis of cultured cells.

Accumulating evidence suggests that soluble Aβ assemblies are formed as intermediates en route to amyloid fibril formation. This scenario is mainly supported by the formation of soluble Aβ assemblies early during the incubation period *in vitro*, which is frequently followed by the appearance of mature fibrils (5, 6, 8, 13). Indeed, certain inhibitors of Aβ fibrillogenesis are potent for blocking the generation of Aβ oligomers (46). In this study, TAβ was preferably formed in the presence of GM1 ganglioside at lower densities than those required for amyloid fibril formation (36). Furthermore, a monoclonal antibody specific to a seed for amyloid fibril formation (40) failed to inhibit TAβ formation. These results suggest that TAβ is formed via a pathway different from a straightforward pathway leading to amyloid fibril formation, as was previously suggested in the formation of other soluble Aβ assemblies (11, 12).

In this study, monomeric Arctic-type Aβ was converted to TAβ more rapidly and to a greater extent than wild-type Aβ. The propensity of Arctic-type Aβ to form toxic nonamyloid Aβ assemblies has recently attracted interest (13, 30, 34); however,

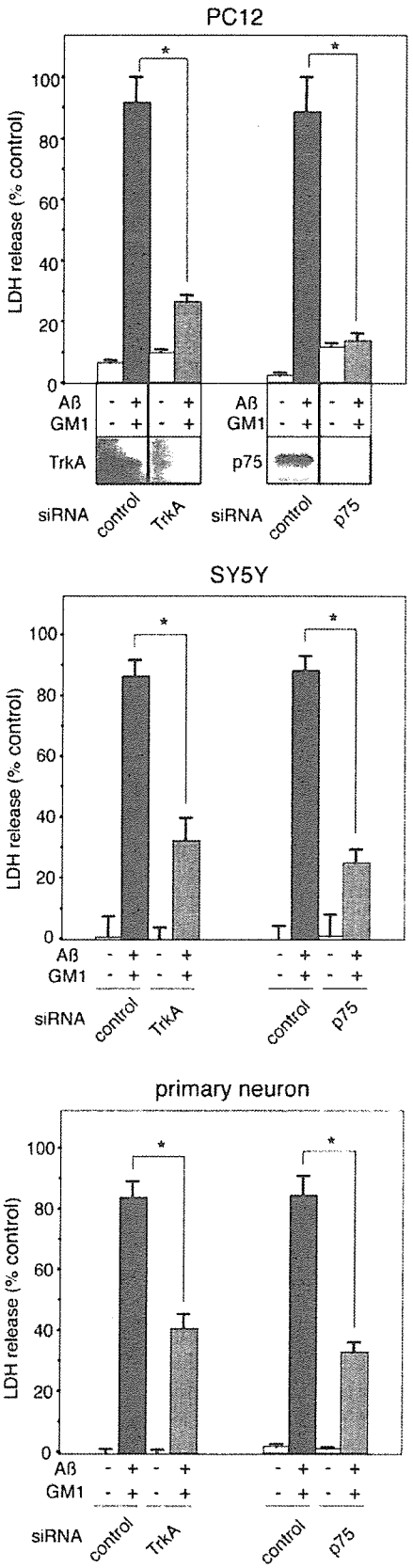

FIGURE 7. **TAβ toxicity mediated by NGF receptors.** PC12 cells, SY5Y cells, and primary neurons, which had been treated with siRNAs against TrkA or $p75^{NTR}$, were exposed to incubation mixtures containing Arctic-type Aβ (Aβ40) at a final concentration of 25 μM, which had been preincubated at 50 μM and 37 °C for 2 h in the absence or presence of 500 μM GM1 ganglioside (the molar ratio of GM1 ganglioside in liposomes was 10%). TAβ toxicity, which was assessed by LDH release assay, was markedly suppressed by the knockdown of TrkA or $p75^{NTR}$. Decreases in TrkA and $p75^{NTR}$ expression levels were confirmed by Western blotting of cell lysates using anti-TrkA and anti-$p75^{NTR}$ antibodies, respectively. Each *column* indicates the average of three values ± S.D. *, $p < 0.0001$.

it remains to be clarified how the assembly of Arctic-type Aβ is accelerated compared with that of wild-type Aβ. We previously found that Aβ fibrillogenesis from Arctic-type Aβ is also enhanced in the presence of SDS as well as GM1 ganglioside (36). Thus, taken together with the results of this study, it is likely that the negatively charged membrane surface is a preferred environment for Arctic-type Aβ to form soluble and insoluble assemblies. A previous study suggested that the lateral distribution of GM1 ganglioside affects the spatial arrangements of the oligosaccharide chain of a molecule (47). Thus, the conformation of GM1 ganglioside may be modulated at certain densities, providing a favorable microenvironment for TAβ formation.

Results of this study imply that GM1 ganglioside potently accelerates the formation of not only amyloid fibrils but also the soluble Aβ assembly. It has recently been reported that Aβ oligomerization is induced in the presence of lipid rafts isolated from brain tissues and cultured cells in a ganglioside-dependent manner (48). Although further studies are necessary, it may be assumed that GM1 ganglioside-rich membrane microdomains, such as lipid rafts, provide a favorable environment that facilitates the formation of soluble Aβ assemblies, including Aβ oligomers and dimers (49).

In this study, the incubation of Arctic-type Aβ with synaptosomes prepared from aged mouse brains markedly induced TAβ formation. Furthermore, the level of GM1 ganglioside significantly increased, whereas that of cholesterol significantly decreased with age. Our observation of an age-dependent alteration in lipid composition of neuronal membranes is in agreement with the result of a recent study of cerebral cortices of AD brains (38). Taking this together with our recent observation that the level of GM1 ganglioside in synaptosomes increases not only with age but also with the expression of apolipoprotein E4 (37), it is possible that TAβ can be formed in the brain in association with the risk factors for AD development.

It was previously reported that Aβ-derived diffusible ligands potently alter NGF-mediated signaling in cultured cells (11). Moreover, many previous studies suggested that Aβ toxicities emerge through the association with $p75^{NTR}$ (50–56) (for a review, see Refs. 57–59). In particular, it is noteworthy that Aβ toxicity mediated by $p75^{NTR}$ depends on a death domain (60) in the cytoplasmic part of $p75^{NTR}$ molecules (56). Evidence indicates the dual function of $p75^{NTR}$: one for survival and the other for death (61) (for a review, see Refs. 57 and 58). Furthermore, a previous study revealed that heteromeric TrkA-$p75^{NTR}$ complexes have different functions from homo-oligomeric TrkA or $p75^{NTR}$ alone (62). Notably, the knockdown of either TrkA or $p75^{NTR}$ is sufficient for suppressing TAβ toxicity. Thus, it may be assumed that the function of heteromeric TrkA-$p75^{NTR}$ complexes is

perturbed by TAβ binding to $p75^{NTR}$ or TrkA, leading to apoptosis through the activation of the death domain of $p75^{NTR}$ (for a review, see Ref. 58). However, it should be noted that conflicting evidence also exists; the expression of $p75^{NTR}$ protects against the toxicity of soluble Aβ assembly or extracellular Aβ (63, 64). These opposite conclusions imply that the signaling pathways of $p75^{NTR}$ are complicated and that the functions of $p75^{NTR}$ vary depending on cell type and context (for a review, see Ref. 57).

To date, various soluble Aβ assemblies with diverse structural features have been detected in a broad range of *in vitro* and *in vivo* studies, which employed different techniques in preparing or isolating such assemblies. As previously reported (11, 65), Aβ assembles into multiple alternative structures. Thus, at this point, it is difficult to determine whether TAβ is identical to or distinct from previously identified soluble Aβ assemblies. However, on the basis of its biophysical features, including its SDS disaggregatability and unsuccessful detection on a carbon-coated grid by EM, TAβ probably differs from previously reported Aβ assemblies, particularly protofibrils, because most protofibrils appear to adsorb equally onto carbon-coated grids (65); moreover, no TAβ is detected by EM under conditions in which protofibrils are readily detected. One interesting soluble Aβ assembly is Aβ*56 (25). Aβ*56 may be a candidate Aβ assembly responsible for plaque-independent cognitive decline in AD; however, its biophysical features, including molecular mass and marked stability in SDS-PAGE, make it distinct from TAβ.

Finally, this study indicates a novel pathological implication of soluble Aβ assemblies. It is well documented that early and severe neuronal loss in the cholinergic basal forebrain in AD is probably responsible for cognitive decline in AD patients. Previous studies suggested that cholinergic phenotype alone is unlikely to be a sufficient condition for inducing neuronal death in AD. Certain cholinergic neurons, such as those in the pontomesencephalon, are unaffected in AD (66). Notably, cholinergic neurons in the pontomesencephalon are free of NGF receptors, whereas those in the basal forebrain, which are early and severely affected in AD, have NGF receptors (67). Taken together, our results suggest that soluble Aβ assemblies, such as TAβ, are responsible for the loss of NGF-dependent neurons in the cholinergic basal forebrain in AD. A future challenge is the production of a monoclonal neutralizing antibody against TAβ toxicity, which would provide promising therapeutic strategies, as suggested by *in vitro* and *in vivo* studies that selectively targeted Aβ oligomers (68, 69).

Acknowledgments—We thank Dr. Matsuzaki for helpful discussion and Dr. Shibata for supplying 4396C.

REFERENCES

1. Terry, R. D., Masliah, E., and Hansen, L. (1999) in *Alzheimer Disease* (Terry, R. D., Katzman, R., Bick, K. L., and Sisodia, S. S. eds) pp. 187–206, Lippincott Williams and Wilkins, Philadelphia, PA
2. Hsia, A. Y., Masliah, E., McConlogue, L., Yu, G. Q., Tatsuno, G., Hu, K., Kholodenko, D., Malenka, R. C., Nicoll, R. A., and Mucke, L. (1999) *Proc. Natl. Acad. Sci. U. S. A.* **96,** 3228–3233
3. Mucke, L., Masliah, E., Yu, G. Q., Mallory, M., Rockenstein, E. M., Tatsuno, G., Hu, K., Kholodenko, D., Johnson-Wood, K., and McConlogue, L. (2000) *J. Neurosci.* **20,** 4050–4058
4. Podlisny, M. B., Ostaszewski, B. L., Squazzo, S. L., Koo, E. H., Rydell, R. E., Teplow, D. B., and Selkoe, D. J. (1995) *J. Biol. Chem.* **270,** 9564–9570
5. Harper, J. D., Wong, S. S., Lieber, C. M., and Lansbury, P. T. (1997) *Chem. Biol.* **4,** 119–125
6. Walsh, D. M., Lomakin, A., Benedek, G. B., Condron, M. M., and Teplow, D. B. (1997) *J. Biol. Chem.* **272,** 22364–22372
7. Lambert, M. P., Barlow, A. K., Chromy, B. A., Edwards, C., Freed, R., Liosatos, M., Morgan, T. E., Rozovsky, I., Trommer, B., Viola, K. L., Wals, P., Zhang, C., Finch, C. E., Krafft, G. A., and Klein, W. L. (1998) *Proc. Natl. Acad. Sci. U. S. A.* **95,** 6448–6453
8. Hartley, D. M., Walsh, D. M., Ye, C. P., Diehl, T., Vasquez, S., Vassilev, P. M., Teplow, D. B., and Selkoe, D. J. (1999) *J. Neurosci.* **19,** 8876–8884
9. Walsh, D. M., Klyubin, I., Fadeeva, J. V., Cullen, W. K., Anwyl, R., Wolfe, M. S., Rowan, M. J., and Selkoe, D. J. (2002) *Nature* **416,** 535–539
10. Dahlgren, K. N., Manelli, A. M., Stine, W. B., Jr., Baker, L. K., Krafft, G. A., and LaDu, M. J. (2002) *J. Biol. Chem.* **277,** 32046–32053
11. Chromy, B. A., Nowak, R. J., Lambert, M. P., Viola, K. L., Chang, L., Velasco, P. T., Jones, B. W., Fernandez, S. J., Lacor, P. N., Horowitz, P., Finch, C. E., Krafft, G. A., and Klein, W. L. (2003) *Biochemistry* **42,** 12749–12760
12. Hoshi, M., Sato, M., Matsumoto, S., Noguchi, A., Yasutake, K., Yoshida, N., and Sato, K. (2003) *Proc. Natl. Acad. Sci. U. S. A.* **100,** 6370–6375
13. Whalen, B. M., Selkoe, D. J., and Hartley, D. M. (2005) *Neurobiol. Dis.* **20,** 254–266
14. Lacor, P. N., Buniel, M. C., Chang, L., Fernandez, S. J., Gong, Y., Viola, K. L., Lambert, M. P., Velasco, P. T., Bigio, E. H., Finch, C. E., Krafft, G. A., and Klein, W. L. (2004) *J. Neurosci.* **24,** 10191–10200
15. Demuro, A., Mina, E., Kayed, R., Milton, S. C., Parker, I., and Glabe, C. G. (2005) *J. Biol. Chem.* **280,** 17294–17300
16. Chong, Y. H., Shin, Y. J., Lee, E. O., Kayed, R., Glabe, C. G., and Tenner, A. J. (2006) *J. Biol. Chem.* **281,** 20315–20325
17. Malaplate-Armand, C., Florent-Bechard, S., Youssef, I., Koziel, V., Sponne, I., Kriem, B., Leininger-Muller, B., Olivier, J. L., Oster, T., and Pillot, T. (2006) *Neurobiol. Dis.* **23,** 178–189
18. Roher, A. E., Chaney, M. O., Kuo, Y. M., Webster, S. D., Stine, W. B., Haverkamp, L. J., Woods, A. S., Cotter, R. J., Tuohy, J. M., Krafft, G. A., Bonnell, B. S., and Emmerling, M. R. (1996) *J. Biol. Chem.* **271,** 20631–20635
19. Kuo, Y.-M., Emmerling, M. R., Vigo-Pelfrey, C., Kasunic, T. C., Kirkpatrick, J. B., Murdoch, G. H., Ball, M. J., and Roher, A. E. (1996) *J. Biol. Chem.* **271,** 4077–4081
20. Pitschke, M., Prior, R., Haupt, M., and Riesner, D. (1998) *Nat. Med.* **4,** 832–834
21. McLean, C. A., Cherny, R. A., Fraser, F. W., Fuller, S. J., Smith, M. J., Beyreuther, K., Bush, A. I., and Masters, C. L. (1999) *Ann. Neurol.* **46,** 860–866
22. Gong, Y., Chang, L., Viola, K. L., Lacor, P. N., Lambert, M. P., Finch, C. E., Krafft, G. A., and Klein, W. L. (2003) *Proc. Natl. Acad. Sci. U. S. A.* **100,** 10417–10422
23. Kayed, R., Head, E., Thompson, J. L., McIntire, T. M., Milton, S. C., Cotman, C. W., and Glabe, C. G. (2003) *Science* **300,** 486–489
24. Cleary, J. P., Walsh, D. M., Hofmeister, J. J., Shankar, G. M., Kuskowski, M. A., Selkoe, D. J., and Ashe, K. H. (2005) *Nat. Neurosci.* **8,** 79–84
25. Lesné, S., Koh, M. T., Kotilinek, L., Kayed, R., Glabe, C. G., Yang, A., Gallagher, M., and Ashe, K. H. (2006) *Nature* **440,** 352–357
26. Oddo, S., Caccamo, A., Tran, L., Lambert, M. P., Glabe, C. G., Klein, W. L., and LaFerla, F. M. (2006) *J. Biol. Chem.* **281,** 1599–1604
27. Ohno, M., Chang, L., Tseng, W., Oakley, H., Citron, M., Klein, W. L., Vassar, R., and Disterhoft, J. F. (2006) *Eur. J. Neurosci.* **23,** 251–260
28. Levy, E., Carman, M. D., Fernandez-Madrid, I. J., Power, M. D., Lieberburg, I., van Duinen, S. G., Bots, G. T., Luyendijk, W., and Frangione, B. (1990) *Science* **248,** 1124–1126
29. Hendriks, L., van Duijn, C. M., Cras, P., Cruts, M., Van Hul, W., van Harskamp, F., Warren, A., McInnis, M. G., Antonarakis, S. E., Martin, J. J., Hofman, A., and Van Broeckhoven, C. (1992) *Nat. Genet.* **1,** 218–221
30. Nilsberth, C., Westlind-Danielsson, A., Eckman, C. B., Condron, M. M.,

Axelman, K., Forsell, C., Stenh, C., Luthman, J., Teplow, D. B., Younkin, S. G., Naslund, J., and Lannfelt, L. (2001) *Nat. Neurosci.* **4,** 887–893
31. Melchor, J. P., McVoy, L., and Van Nostrand, W. E. (2000) *J. Neurochem.* **74,** 2209–2212
32. Grabowski, T. J., Cho, H. S., Vonsattel, J. P., Rebeck, G. W., and Greenberg, S. M. (2001) *Ann. Neurol.* **49,** 697–705
33. Cheng, I. H., Palop, J. J., Esposito, L. A., Bien-Ly, N., Yan, F., and Mucke, L. (2004) *Nat. Med.* **10,** 1190–1192
34. Lashuel, H. A., Hartley, D., Petre, B. M., Walz, T., and Lansbury, P. T., Jr. (2002) *Nature* **418,** 291
35. Yanagisawa, K., Odaka, A., Suzuki, N., and Ihara, Y. (1995) *Nat. Med.* **1,** 1062–1066
36. Yamamoto, N., Hasegawa, K., Matsuzaki, K., Naiki, H., and Yanagisawa, K. (2004) *J. Neurochem.* **90,** 62–69
37. Yamamoto, N., Igbabvoa, U., Shimada, Y., Ohno-Iwashita, Y., Kobayashi, M., Wood, W. G., Fujita, S. C., and Yanagisawa, K. (2004) *FEBS Lett.* **569,** 135–139
38. Molander-Melin, M., Blennow, K., Bogdanovic, N., Dellheden, B., Manssson, J. E., and Fredman, P. (2005) *J. Neurochem.* **92,** 171–182
39. Gylys, K. H., Fein, J. A., Yang, F., Miller, C. A., and Cole, G. M. (2007) *Neurobiol. Aging* **28,** 8–17
40. Hayashi, H., Kimura, N., Yamaguchi, H., Hasegawa, K., Yokoseki, T., Shibata, M., Yamamoto, N., Michikawa, M., Yoshikawa, Y., Terao, K., Matsuzaki, K., Lemere, C. A., Selkoe, D. J., Naiki, H., and Yanagisawa, K. (2004) *J. Neurosci.* **24,** 4894–4902
41. Maeda, S., Sahara, N., Saito, Y., Murayama, S., Ikai, A., and Takashima, A. (2006) *Neurosci. Res.* **54,** 197–201
42. Hansma, H. G., Laney, D. E., Bezanilla, M., Sinsheimer, R. L., and Hansma, P. K. (1995) *Biophys. J.* **68,** 1672–1677
43. Schroeder, F., Morrison, W. J., Gorka, C., and Wood, W. G. (1988) *Biochim. Biophys. Acta* **946,** 85–94
44. Atwood, C. S., Scarpa, R. C., Huang, X., Moir, R. D., Jones, W. D., Fairlie, D. P., Tanzi, R. E., and Bush, A. I. (2000) *J. Neurochem.* **75,** 1219–1233
45. Bitan, G., Lomakin, A., and Teplow, D. B. (2001) *J. Biol. Chem.* **276,** 35176–35184
46. Walsh, D. M., Townsend, M., Podlisny, M. B., Shankar, G. M., Fadeeva, J. V., Agnaf, O. E., Hartley, D. M., and Selkoe, D. J. (2005) *J. Neurosci.* **25,** 2455–2462
47. Brocca, P., Berthault, P., and Sonnino, S. (1998) *Biophys. J.* **74,** 309–318
48. Kim, S. I., Yi, J. S., and Ko, Y. G. (2006) *J. Cell. Biochem.* **99,** 878–889
49. Kawarabayashi, T., Shoji, M., Younkin, L. H., Wen-Lang, L., Dickson, D. W., Murakami, T., Matsubara, E., Abe, K., Ashe, K. H., and Younkin, S. G. (2004) *J. Neurosci.* **24,** 3801–3809
50. Rabizadeh, S., Bitler, C. M., Butcher, L. L., and Bredesen, D. E. (1994) *Proc. Natl. Acad. Sci. U. S. A.* **91,** 10703–10706
51. Yaar, M., Zhai, S., Pilch, P. F., Doyle, S. M., Eisenhauer, P. B., Fine, R. E., and Gilchrest, B. A. (1997) *J. Clin. Invest.* **100,** 2333–2340
52. Kuner, P., Schubenel, R., and Hertel, C. (1998) *J. Neurosci. Res.* **54,** 798–804
53. Yaar, M., Zhai, S., Fine, R. E., Eisenhauer, P. B., Arble, B. L., Stewart, K. B., and Gilchrest, B. A. (2002) *J. Biol. Chem.* **277,** 7720–7725
54. Perini, G., Della-Bianca, V., Politi, V., Della Valle, G., Dal-Pra, I., Rossi, F., and Armato, U. (2002) *J. Exp. Med.* **195,** 907–918
55. Tsukamoto, E., Hashimoto, Y., Kanekura, K., Niikura, T., Aiso, S., and Nishimoto, I. (2003) *J. Neurosci. Res.* **73,** 627–636
56. Costantini, C., Rossi, F., Formaggio, E., Bernardoni, R., Cecconi, D., and Della-Bianca, V. (2005) *J. Mol. Neurosci.* **25,** 141–156
57. Dechant, G., and Barde, Y. A. (2002) *Nat. Neurosci.* **5,** 1131–1136
58. Lad, S. P., Neet, K. E., and Mufson, E. J. (2003) *Curr. Drug Targets CNS Neurol. Disord.* **2,** 315–334
59. Coulson, E. J. (2006) *J. Neurochem.* **98,** 654–660
60. Bothwell, M. (1996) *Science* **272,** 506–507
61. Mamidipudi, V., and Wooten, M. W. (2002) *J. Neurosci. Res.* **68,** 373–384
62. Lad, S. P., Peterson, D. A., Bradshaw, R. A., and Neet, K. E. (2003) *J. Biol. Chem.* **278,** 24808–24817
63. Costantini, C., Della-Bianca, V., Formaggio, E., Chiamulera, C., Montresor, A., and Rossi, F. (2005) *Exp. Cell Res.* **311,** 126–134
64. Zhang, Y., Hong, Y., Bounhar, Y., Blacker, M., Roucou, X., Tounekti, O., Vereker, E., Bowers, W. J., Federoff, H. J., Goodyer, C. G., and LeBlanc, A. (2003) *J. Neurosci.* **23,** 7385–7394
65. Lashuel, H. A., Hartley, D. M., Petre, B. M., Wall, J. S., Simon, M. N., Walz, T., and Lansbury, P. T., Jr. (2003) *J. Mol. Biol.* **332,** 795–808
66. Woolf, N. J., Gould, E., and Butcher, L. L. (1989) *Neuroscience* **30,** 143–152
67. Woolf, N. J., Jacobs, R. W., and Butcher, L. L. (1989) *Neurosci. Lett.* **96,** 277–282
68. Lambert, M. P., Viola, K. L., Chromy, B. A., Chang, L., Morgan, T. E., Yu, J., Venton, D. L., Krafft, G. A., Finch, C. E., and Klein, W. L. (2001) *J. Neurochem.* **79,** 595–605
69. Lee, E. B., Leng, L. Z., Zhang, B., Kwong, L., Trojanowski, J. Q., Abel, T., and Lee, V. M. (2006) *J. Biol. Chem.* **281,** 4292–4299

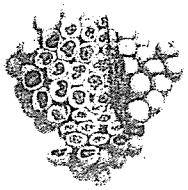

STEM CELLS®

Electrical stimulation modulates fate determination of differentiating embryonic stem cells

Masahisa Yamada, Kentaro Tanemura, Seiji Okada, Akio Iwanami, Masaya Nakamura, Hideaki Mizuno, Michiru Ozawa, Ritsuko Ohyama-Goto, Naohito Kitamura, Masako Kawano, Kyoko Tan-Takeuchi, Chiho Ohtsuka, Atsushi Miyawaki, Akihiko Takashima, Masaharu Ogawa, Yoshiaki Toyama, Hideyuki Okano and Takashi Kondo

Stem Cells published online Nov 16, 2006;
DOI: 10.1634/stemcells.2006-0011

Stem Cells Express, published online November 16, 2006; doi:10.1634/stemcells.2006-0011

Embryonic Stem Cells

Electrical stimulation modulates fate determination of differentiating embryonic stem cells

Masahisa Yamada[a,b], Kentaro Tanemura[c,d], Seiji Okada[f], Akio Iwanami[f], Masaya Nakamura[g], Hideaki Mizuno[e], Michiru Ozawa[c], Ritsuko Ohyama-Goto[c], Naohito Kitamura[b], Masako Kawano[a], Kyoko Tan-Takeuchi[a], Chiho Ohtsuka[c], Atsushi Miyawaki[e], Akihiko Takashima[d], Masaharu Ogawa[a], Yoshiaki Toyama[g], Hideyuki Okano[f] and Takashi Kondo[c*]

[a]*Laboratory for Cell Culture Development;* [b]*Yamada Research Unit, Molecular Neuropathology Group;* [c]*Kondo Research Unit, Brain Development Research Group;* [d]*Laboratory for Alzheimer's Disease; and* [e]*Laboratory for Cell Function Dynamics, Brain Science Institute, Institute of Physical and Chemical Research (RIKEN), 2-1 Hirosawa, Wako, Saitama 351-0198, Japan;* [f]*Department of Physiology; and* [g]*Department of Orthopaedic Surgery, Keio University School of Medicine, 35 Shinanomachi, Shinjuku-ku, Tokyo 160-8582, Japan*

Received on January 6, 2006; accepted for publication on November 8, 2006.
 1066-5099 doi: 10.1634/stemcells.2006-0011

Key Words. ES cell, neuron, Tissue regeneration, calcium flux

Running Title: Electrical stimulation induces neuronal fate

*To whom correspondence should be addressed:

Takashi Kondo,
email: TKondo@brain.riken.jp
TEL: +81-48-467-6729
FAX: +81-48-467-6729

Abstract

A clear understanding of cell fate regulation during differentiation is key in successfully using stem cells for therapeutic applications. Here, we report that mild electrical stimulation strongly influences embryonic stem cells to assume a neuronal fate. Although the resulting neuronal cells showed no sign of specific terminal differentiation in culture, they showed potential to differentiate into various types of neurons *in vivo,* and in adult mice contributed to the injured spinal cord as neuronal cells. Induction of calcium ion influx is significant in this differentiation system. This phenomenon opens up possibilities for understanding novel mechanisms underlying cellular differentiation and early development, and perhaps more importantly, suggests possibilities for treatments in medical contexts.

Introduction

Embryonic stem (ES) cells are pluripotent cells that can, *in vivo* and *ex vivo,* give rise to cells of different fates. Through induction, ES cells form embryoid bodies (EBs); and in this way, ES cells are capable of differentiating into a variety of tissue types, such as extraembryonic endoderm and neural and muscle tissue, and so on [1-3]. Many growth factors and signaling pathways initiate differentiation and modulate the course of cellular differentiation [4-7]. Several reports show that, with the application of certain growth factors or the alteration of culture conditions, ES cells can differentiate in a relatively efficient manner into specific neuronal cell types that are destined to become certain neuronal tissues [5,8-11].

Another important factor that possibly influences developmental processes and is central for cellular homeostasis is transmembrane ion distribution. Unequal distributions of ions between the intra- and extracellular compartments yield electrical potential, which is crucial for neural transmission. Ions also play a role in shaping neuronal circuits during development via neural transmission; ions induce functional and structural refinement of synapses and neuronal networks by modulating activity-

dependent gene transcription [12,13]. Despite the important role of ionic density in development, very little information is available on the roles of intra- and extracellular ionic density in cell-fate determination. Here, we report that electrical stimulation can bias the fate of differentiating ES cells towards neuronal lineages. Growth factor-induced ES cells usually differentiate into rather restricted neuronal cell types. In contrast, electrically induced ES cells that ultimately differentiate into neurons are plastic in their capacity to differentiate into a wide variety of specific cell types. These ES cells are pluripotent, capable of differentiating into any neuronal lineage found within the various neuronal tissue types we examined.

Materials and Methods

Fluorescent ES cells

Venus-expressing ES cells were prepared by transfecting R1 ES cells with a construct containing Venus driven by a CAGGS promoter. R1 ES cells were a generous gift from Dr. Andreas Nagy. The Venus construct was made from plasmids kindly provided by Dr. Jun-ichi Miyazaki [14,15].

Differentiation method in cell culture

The protocol for ES cell differentiation is schematized in Figure 1. Embryoid bodies (EBs) were made by culturing R1 ES cells with DMEM containing 10% FCS without leukemia inhibitory factor (LIF) in non-coated bacterial petri dishes (Nunc). After 3 days of culture, electrical stimulation was applied to cells in a 4-mm gap cuvette under several voltage conditions (0V, 5V, 10V, and 20V; see supplemental data). One train of 5 pulses (950-ms inter-pulse interval) was delivered with an electroporater (CUY21E; Tokiwa Science). For cell culture experiments, stimulated EBs were maintained in DMEM with 10% FCS (GIBCO) on poly-D-Lysine-coated plates (BD). Ten days after

stimulation, cells were fixed in paraformaldehyde in phosphate buffered saline (pH 7.4) for immunocytochemical analyses. For animal experiments, Venus-positive EBs were stimulated similarly (10 V, same 5-pulse train) and then dissociated with trypsin-EDTA for 3 min. Dissociated cells were injected into either mouse embryos or adult spinal cords.

Immunostaining

Cultured cells or histological sections were processed for immunostaining using the following antibodies: anti-TuJ1 mouse monoclonal antibody (mAb) (1:500; BAbCO), anti-GFP rat mAb (Nacalai), anti-Hu human pAb (1:1000; a generous gift from Dr. Robert Darnell), anti-Ki67 rat mAb (DAKO), anti-MAP2 mouse mAb (1:200; Chemicon), anti-ChAT rabbit pAb (1:200; Chemicon), anti-Islet1 mAb (1:400; DSHB), anti-Pax6 mAb (1:200; DSHB), anti-Pax7 mAb (1:400; DSHB), anti-MNR2 mAb (1:400; DSHB), and anti-Nkx2.2 mAb (1:400; DSHB). Histological sections were stained with the protocol described previouly [16], and immunostained images were obtained with an LSM-510 confocal laser microscope (Carl Zeiss, Germany) by

sequential scanning and analyzed with adjunctive software attached to the LSM-510. The thickness of the histological sections was less than 7 μm, and the z-axis sampling of the confocal images was less than 1 μm.

Measurement of intracellular Ca^{2+} concentration

ES cells or EBs were loaded with the Ca^{2+} fluorescence indicator fura-2 by incubating the cells in Hank's balanced salt solution (HBSS) containing 2 μM fura-2 AM (Molecular Probes) and 0.01% cremophor-EL (Sigma) at room temperature for 30 min. After loading, cells were washed in fresh HBSS and incubated an additional 15+ min prior to analysis of intracellular Ca^{2+} concentration ($[Ca^{2+}]_i$). $[Ca^{2+}]_i$ was analyzed with an inverted fluorescent microscope (IX-70, Olympus) equipped with a filter exchanger (Lambda 10-2, Sutter Instruments) and a cooled charge-coupled device camera (MicroMax, Roper Scientific). One train of 5 pulses (950-ms inter-pulse interval) was delivered with an electroporater (CUY459G20; Neppagene). The following optics were used: excitation filter, 340HT15 and 380HT15 (Omega Optics); dichroic mirror, 430DCLP (Omega Optics); emission filter, 510WT40 (Omega Optics); objective lens,

Uapo/340 20x/0.75 (Olympus). Metafluor 5.0 software (Universal Imaging) was used to control the system and analyze acquired images [17].

Spinal Cord Injury Model

Spinal cord injury was induced with a modified NYU impactor as described previously [18]. Briefly, female C57BL/6J mice were anesthetized with an intraperitoneal injection of ketamine (100 mg/kg) and xylazine (10 mg/kg). After laminectomy at the T9 level, the dorsal surface of the dura matter was exposed. The vertebral column was stabilized with fine forceps and clamps at the T7 and T10 spinous processes and ligament, and then the animal's body was lifted. A 3-g weight (1.2-mm-diameter tip) was allowed to drop from a height of 25 mm onto the dorsal surface of the dura matter. The muscles and the incision were then closed in layers, and the animals were placed in a temperature-controlled chamber until thermoregulation was reestablished. Manual bladder evacuation was performed twice per day until reflex bladder emptying was reestablished.

Results

Cell fate determination of electrically stimulated cells in culture

We examined the influence of inter- and intracellular ionic balance on differentiation fate by application of weak electrical pulses. Embryoid bodies (EBs) were stimulated at one of several intensities via an electrode (Fig. 1). The EBs were cultured for 10 days, then fixed to assess differentiation fate (Fig. 1). Assessment for various markers (i.e., mainly for muscle and neural tissue) indicated that R1 ES cells showed no neuronal or myocytic differentiation, regardless of whether they were electrically stimulated (Fig. 2A, 2B, 2M, and 2N). In contrast, EBs receiving electrical stimulation showed robust neuronal differentiation; control EBs (i.e., those receiving no stimulation) showed little differentiation (Fig. 2). Almost all colonies of EBs receiving 10 V stimulation contained cells immunoreactive for TuJ1, a marker for early committed neuronal cells, whereas less than 10% of control colonies contained TuJ1-positive cells derived from EBs receiving zero-volt stimulation (Fig. 2A and 2C). We confirmed the neuronal identity of the cells from colonies that received 10 V stimulation: the majority of these cells were MAP2 immunoreactive (Supplemental Fig. s1), while 20-30% of cells showed immunoreactive to MAP2 by retinoid treatment.

It is noteworthy that the neuronal cells in our system differentiated in a significantly shorter time than those in most of other systems that use growth factors to initiate cell differentiation [5,10,11]. The differentiation efficiency slightly decreased in cells that received 20 V stimulation compared to that in cells that received milder stimulation. Although the morphology of these cells also clearly differed (e.g., thicker dendritic processes than the ones receiving milder stimulation), all expressed TuJ1 (Fig. 2J). The size and number of colonies produced from cells stimulated with 20 V did not clearly differ from the size and number of colonies produced from the unstimulated cells. The size and number of colonies produced from cells stimulated with 5-15 V also did not differ. We note that the cell number and cell death did not show significant difference among EBs with or without electrical stimulation after outgrowth on the poly-D-Lysine plate (tunnel assay showed 11-13% of cell death at 1 days and 3 days after outgrowth of EBs with electrical stimulation and without stimulation).

In general, we observed few muscle progenitors as a result of electrical stimulation, even though a slight but insignificant, increase in muscle progenitors was observed for EBs receiving 5-V stimulation (Fig. 2B, 2D). In addition, we did not observe cells